

# Highly Efficient Intrinsic Phosphorescence from a $\sigma$ -Conjugated Poly(silylene) Polymer

A. Kadashchuk,<sup>\*,†,‡</sup> Yu. Skryshevski,<sup>†</sup> A. Vakhnin,<sup>†</sup> S. Toliautas,<sup>§</sup> J. Sulskus,<sup>§</sup> R. Augulis,<sup>||</sup> V. Gulbinas,<sup>⊥,||</sup> S. Nespurek,<sup>#</sup> J. Genoe,<sup>‡</sup> and L. Valkunas<sup>§,||</sup>

<sup>†</sup>Institute of Physics, National Academy of Sciences of Ukraine, Prospect Nauky 46, 03028 Kyiv, Ukraine

<sup>‡</sup>IMEC, Kapeldreef 75, B-3001 Leuven, Belgium

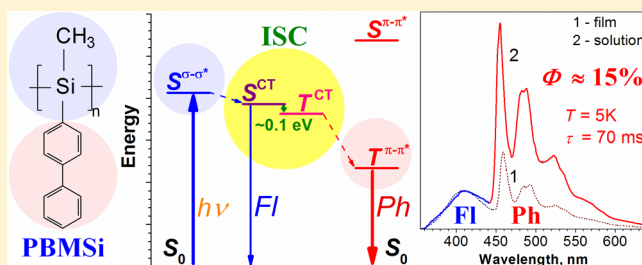
<sup>§</sup>Department of Theoretical Physics and <sup>⊥</sup>Department of General Physics and Spectroscopy, Faculty of Physics, Vilnius University, Saulėtekio 9-III, LT-10222 Vilnius, Lithuania

<sup>||</sup>Center for Physical Sciences and Technology, Savanorių 231, LT-02300 Vilnius, Lithuania

<sup>#</sup>Department of Material Research, Regional Innovation Centre for Electrical Engineering (RICE), Faculty of Electrical Engineering, University of West Bohemia, 306 14 Pilsen, Czech Republic

## Supporting Information

**ABSTRACT:** We have observed highly efficient intrinsic phosphorescence of a neat  $\sigma$ -conjugated polymer, poly(biphenyl-4-ylmethylsilylene) (PBMSi). At low temperatures, PBMSi solid films featured  $\sim 15\%$  phosphorescence quantum yield, which is unusually high for purely organic conjugated polymers and is comparable to that of organometallic polymers. Exciton dynamics in PBMSi was studied by ultrafast fluorescence and time-gated delayed emission measurements. It was shown that the phosphorescence of PBMSi originates from the radiative decay of triplets on the  $\pi$ -conjugated biphenyl group constituting the lowest triplet state,  $T_1$ , which is populated under the excitation of the  $\sigma$ -conjugated polymer backbone, i.e., with energy well below the lowest singlet excited state of the biphenyl group itself. The nature of the excited states in PBMSi was further investigated by performing quantum-mechanical calculations of the model compound. The calculations showed that the lowest singlet excited state has charge-transfer (CT) character involving different parts of the same macromolecule. Energetically this state lies very close to the CT triplet excited state. We argue that the intramolecular CT state is responsible for the strongly enhanced intersystem crossing (ISC) in PBMSi due to the small positive CT singlet–triplet energy splitting, which is itself a consequence of a weak exchange interaction of a spatially separated electron and hole in the CT state. This study suggests a new molecular-level engineering approach for enhancement of the ISC, enabling efficient conversion of primary excited singlets into triplets in conjugated polymers without involving a heavy atom effect while leaving the rate of radiative  $T_1 \rightarrow S_0$  transition virtually unaffected.



## INTRODUCTION

Phosphorescence (Ph), i.e., radiative decay of the triplet excited state to the singlet ground state, is usually very weak in most light-emitting materials and thus difficult to detect unless the emitter contains heavy atoms that enhance the spin–orbit coupling.<sup>1–3</sup> This coupling ensures efficient conversion of primarily generated singlet states into triplets and, more importantly, makes the spin-forbidden  $T_1 \rightarrow S_0$  transition partially allowed, resulting in the enhancement of the Ph intensity. The spin–orbit coupling is realized in so-called triplet emitter compounds, such as Pt- or Ir-containing organometallic complexes<sup>2,4</sup> or Pt-containing conjugated polymers.<sup>5–7</sup> In organic semiconductors the combination of low intersystem crossing (ISC) rate implying low population of the triplet state, low radiative rate, and high nonradiative decay results in an extremely low phosphorescence yield for materials devoid of heavy atoms. The reported Ph yield for conjugated polymers is

usually as small as  $10^{-4}$  (established for methyl-substituted ladder-type poly(*p*-phenylene) (MeLPPP), a benchmark  $\pi$ -conjugated polymer); therefore, one has to use time-gated spectroscopy techniques to detect such extremely weak emission.<sup>8</sup> For some classes of conjugated polymers, for example, poly(phenylenevinylene) (PPV)-type polymers, the Ph emission is not detectable at all due to strong nonradiative quenching, unless special methods of sensitization of Ph in PPV derivatives are applied by doping the polymer with suitable organometallic complexes.<sup>9</sup>

On the other hand, the interest in the Ph phenomena in organic semiconductors has greatly increased during the past decade due to creation of highly efficient phosphorescent

Received: July 12, 2014

Revised: September 3, 2014

Published: September 8, 2014

organic light-emitting diodes (OLEDs) with internal quantum efficiency approaching 100%.<sup>2</sup> Organic electrophosphorescent devices normally employ organometallic guest molecules (triplet emitters) which can harvest both singlet and triplet electrogenerated excitons. For efficient electrophosphorescence from triplet guests in a host matrix, the triplet energy of the host has to be higher than that of the guest to facilitate exothermic energy transfer from the host to the guest and to prohibit reverse energy transfer from the guest back to the host (i.e., to effectively confine triplet excitons on guest molecules). Among the reported host materials, carbazole derivatives are the most popular.<sup>10</sup> Carbazole-based materials simultaneously possess large enough energies and reasonable charge carrier mobility. There is, however, a need for polymers possessing a high energy triplet state and better charge transport properties. Such conjugated polymers could potentially be promising for creation of white-light-emitting polymer OLEDs<sup>11</sup> which, despite currently still exhibiting worse performance compared to small-molecule OLEDs, should be favorable due to the possibility of depositing them by efficient wet-coating technologies.

High population of the triplet state due to efficient ISC upon optical excitation of an organic film is critical for novel applications, such as noncoherent up-conversion by triplet–triplet annihilation (TTA-UC).<sup>12–14</sup> The latter can be used for the enhancement of the light-harvesting efficiency of solar cells by converting low-energy photons not otherwise absorbed by the semiconductor into higher energy photons and for biomedical applications in photodynamic therapy. For pristine conjugated polymers the ISC efficiency is very low,<sup>3</sup> typically less than 1% (the ISC yield of 0.2% was estimated for MeLPPP); therefore, the achievement of substantial triplet population in them inevitably requires sensitization by triplet emitter compounds.

Besides the strength of the spin–orbit coupling, another important factor for the intersystem crossing rate is the vibrational overlap between the wave functions of the singlet and triplet states involved, and it depends strongly on the energy difference between these states,  $\Delta E_{ST}$  (singlet–triplet splitting energy). In materials of small molecular weight, the  $\Delta E_{ST}$  can be significantly reduced using an appropriate molecular substitution,<sup>15</sup> thus resulting in a strong enhancement of the ISC. In conjugated polymers, however, the singlet–triplet splitting has been experimentally found to be fairly large, around 0.7 eV;<sup>16</sup> that does not favor the ISC rate. On the other hand, it was demonstrated that singlet and triplet energy levels should be more closely spaced in the case of intermolecular (off-chain) charge-transfer (CT) states<sup>3,12,17</sup> compared to the neutral excitons, which would promote the ISC rates between these levels. It should be mentioned that recent progress in the design of organic molecules with intramolecular CT within systems containing spatially separated donor and acceptor moieties has resulted in the development of a new class of metal-free organic molecules which feature a remarkably small  $\Delta E_{ST}$  (typically <0.1 eV).<sup>18</sup> In addition to the enhanced ISC, an efficient  $T_1 \rightarrow S_1$  reverse intersystem crossing (RISC) of triplet excitons could be obtained in such molecules just by thermal up-conversion to singlets at ambient temperature, thus enabling efficient thermally activated delayed luminescence (TADF).<sup>18–22</sup> The molecules exhibiting TADF are currently attracting considerable attention as highly efficient fluorescence emitters for OLED applications because of the high (reaching almost 100%) electroluminescence yield.<sup>18</sup> Such materials can

potentially eliminate the need for expensive phosphorescent compounds containing rare metals such as Ir or Pt.

In the present paper we report a surprisingly efficient intrinsic Ph due to strongly enhanced ISC found in a neat poly(biphenyl-4-ylmethylsilylene) (PBMSi)  $\sigma$ -conjugated polymer, featuring a quantum yield as large as  $\sim 15\%$  in solid films, which is comparable to that of organometallic polymers. Poly(silylene)s (also found in various literature under the names of polysilanes, poly(organosilane)s, poly-(organylsilylene)s, organopolysilanes, poly(organylsilanediy)s, or catena silicon polymers) belong to the class of  $\sigma$ -conjugated polymers with a silicon polymer backbone, whose electronic properties are attributed to the  $\sigma$ -conjugation originating from the overlap of Si  $sp^3$  orbitals.<sup>23–25</sup> The optical and electrical properties of these polymers differ significantly from those of structurally analogous carbon-based  $\sigma$ -bound systems such as polystyrene and polyethylene, resembling rather fully  $\pi$ -conjugated systems, for example, polyacetylenes. The lowest energy optically allowed excited state of poly(silylene)s was found to be of the excitonic nature,<sup>25</sup> principally similar to Frenkel-type excitons in molecular crystals.<sup>3</sup> Poly(silylene)s are typically wide-gap semiconducting polymers, which makes them promising for UV- and white-light OLED applications.<sup>26,27</sup> To clarify the photophysics in this polymer, detailed spectroscopic investigations of PBMSi together with the relevant quantum-mechanical calculations are carried out. The obtained results demonstrate that Ph originates from the radiative decay of triplets on the  $\pi$ -conjugated biphenyl side groups under the excitation of the  $\sigma$ -conjugated polymer backbone, i.e., with energy well below the lowest singlet state of the biphenyl group, while the delayed fluorescence (DF) comes from the polymer backbone as a result of triplet–triplet annihilation. We argue that the exceptionally strong Ph in this polymer results from a greatly increased efficiency of the intersystem crossing between singlet and triplet *intramolecular* charge-transfer states involving the  $\sigma$ -conjugated polymer backbone and  $\pi$ -conjugated biphenyl group of the same PBMSi macromolecule. The biphenyl group constitutes the lowest triplet state ( $T_1^{\pi-\pi^*}$ ) of PBMSi.

## ■ EXPERIMENTAL AND THEORETICAL METHODS

**Materials.** The molecular structure of PBMSi is illustrated in the inset in Figure 1. PBMSi was synthesized by sodium-mediated Wurtz coupling of biphenyl-4-ylmethylchlorosilane in boiling toluene. Butyllithium was added to the system 1 h after the components were mixed. Then the remaining sodium was reacted with ethanol, and the solution formed in this way was washed out with water and dried. PBMSi was then precipitated by adding 2-propanol and purified by several reprecipitations from tetrahydrofuran solution with 2-propanol. The final product was bimodal, consisting of high and middle molecular parts. The high molecular weight fraction remaining after extraction with diethyl ether corresponds to a monomer conversion of about 40%. Its average molar mass,  $M_w = 1.6 \times 10^5 \text{ g mol}^{-1}$ , was determined by the light scattering method and by gel permeation chromatography ( $M_w/M_n = 2$ ). To check the purity of the polymer, the  $^1\text{H}$  NMR spectrum was measured. The ratio of areas of the signals corresponding to aromatic protons and methyl protons was in accordance with the ratio of the number of protons arising from the chemical structure of the polymer. According to X-ray analysis, the final product contained 16% crystalline phase. It was eliminated by heating

the material above the glass temperature, 462 K (the value was determined by differential scanning calorimetry).<sup>28,29</sup>

Small molecular weight compounds of carbazole and naphthalene were employed as dopants in PBMSi for the studies of the triplet energy transfer. They were purified by the zone-refining technique (more than 100 zones) before use. Films of neat polymers were prepared from toluene solution by drop casting. In the case of doped films, the polymer and dopants were dissolved separately in tetrahydrofuran (THF), then the solutions were mixed and stirred for several hours, and the resulting solutions were cast on a fused silica substrate. The concentration of the solution used for coating was 5–10 wt %, which resulted in a film thickness of several micrometers. After deposition, the films were dried at  $10^{-3}$  Pa at room temperature for at least 4 h.

**Spectroscopy Techniques.** Techniques used during the experiments are described in the Supporting Information (section 1).

**Quantum-Mechanical Calculations.** Structure optimization and electronic spectrum calculations of the MSi15-BP oligomer and its moieties—pentadecakis(dimethylsilane) (MSi15) and biphenyl (BP)—were performed using the Gaussian09 package.<sup>30</sup> For the optimization of the geometric parameters in the ground electronic state  $S_0$ , the density functional theory (DFT) approach<sup>31</sup> with the hybrid B3LYP functional<sup>32</sup> and 6-31G(d,p) basis set<sup>33</sup> was used. The time-dependent density functional theory (TD-DFT) method<sup>34</sup> was used at the same computational level to investigate the electronic structure of the 12 lowest singlet ( $S_i$ ) and 12 triplet ( $T_i$ ) excited states.

For the validation of the wave function character of the excited states, additional calculations were carried out using the GAMESS-US computer program<sup>35</sup> at the level of ab initio general multiconfigurational quasi-degenerate perturbation theory (GMC-QDPT<sup>36</sup>) with the 6-31G(d,p) basis set. The comparison between TD-DFT and GMC-QDPT results can be found in the Supporting Information (section 2). The active space of the highest six occupied and the lowest six virtual molecular orbitals was taken into consideration, and multi-reference configurations of up to the fourth excitation order were included during the GMC-QDPT calculations. Eight lowest singlet and eight triplet excited states were considered. Transition dipole moments between these electronic states were also obtained from the GMC-QDPT results, and the radiative transition lifetimes ( $\tau$ ) were estimated by using the following expression:

$$\frac{1}{\tau} = \frac{4\alpha_0^3}{3t_0} (\Delta E)^3 \sum_i |M_i|^2 \quad (1)$$

where  $t_0 = (4\pi\epsilon_0)^2 \hbar^3 / m_e e^4$ ,  $\alpha_0$  is the fine structure constant,  $\Delta E$  is the transition energy between the initial and final states, and  $M_i$  is the projection of the transition dipole moment between the two states. Finally, GAMESS-US was used for the TD-DFT-based optimization of the structures in the  $S_1$ ,  $S_2$ , and  $T_1$  excited states at the LC-BOP/6-31G(d,p) computational level.<sup>37</sup> Potential energy values of the ground ( $S_0$ ), lowest triplet ( $T_1$ ), charge-transfer ( $S^{CT}$ ), and most optically active ( $S^{\sigma-\sigma^*}$ ) states of the MSi15-BP oligomer for the different structural conformations— $S^X$  (intersection of  $S^{\sigma-\sigma^*}$  and  $S^{CT}$  states) and  $S^{CT}_{min}$  and  $T_1^{min}$  (optimized structures of the respective electronic states)—were considered. The geometric

parameters and total energies of the four investigated conformations are presented in the Supporting Information (Tables S1–S4).

## EXPERIMENTAL RESULTS

**Steady-State Spectroscopy of PBMSi.** Figure 1 features absorption and emission spectra of PBMSi measured in diluted

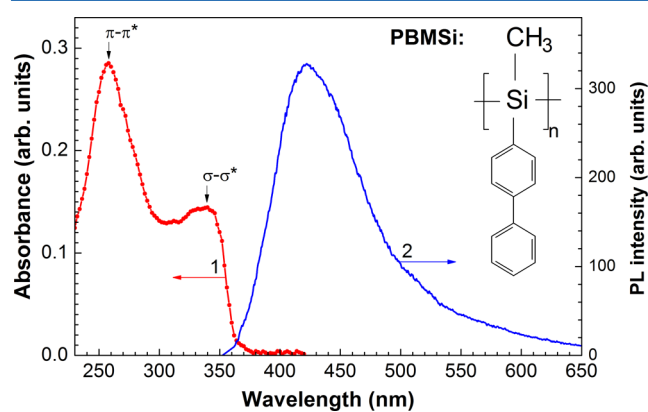


**Figure 1.** Absorption spectrum of PBMSi in dichloromethane solution ( $c = 0.002$  g/L) (curve 1) and the steady-state PL spectrum (curve 2) under 313 nm excitation at room temperature. The inset shows the molecular structure of PBMSi.

dichloromethane solution at room temperature. The absorption spectrum consists of two main peaks at about 340 nm (3.65 eV) and 258 nm (4.81 eV). The longest wavelength absorption band of substituted poly(silylene)s arises from the delocalized  $\sigma-\sigma^*$  transition within the polymer Si backbone.<sup>23,38</sup> The absorption peak at 258 nm is associated with the  $\pi-\pi^*$  transition in the biphenyl side group.<sup>39</sup> The continuous wave photoluminescence (cw-PL) spectra (Figure 1, curve 2) of PBMSi feature a broad structureless band peaking at around 422 nm (2.94 eV) at room temperature. It should be noted that the cw-PL spectrum of PBMSi is strongly bathochromically shifted with respect to the lowest energy absorption band at 340 nm.

It is intriguing that the PL spectra of the PBMSi polymer (in both the solution and film) manifest a striking change upon lowering the temperature. Figure 2a depicts cw-PL spectra of a PBMSi film measured at different temperatures ranging from 5 to 295 K, obtained using a 313 nm light source corresponding to the  $\sigma-\sigma^*$  absorption band. The low-temperature PL spectra clearly show two different spectral components: (1) a broad structureless band peaking at 416 nm (2.98 eV) (hereafter called the “broad band”), which dominates the PL emission at room temperature (cf. Figure 1), and (2) a red-shifted well-structured narrow spectrum (hereafter called the “structured narrow spectrum”) with the shortest wavelength peak at 460 nm (2.7 eV, fwhm  $\approx 800$   $\text{cm}^{-1}$ ) superimposed with the low-energy tail on the broad PL band. The structured narrow spectrum emerges in the cw-PL spectra of PBMSi films at sufficiently low temperatures ( $T \leq 80$  K), and its intensity increases strongly with the lowering of the temperature. No such structured features can be observed in cw-PL spectra of PBMSi films at  $T > 100$  K, while the broad structureless PL band shows just a moderate decrease (approximately by a factor of 1.5) with increasing temperature (Figure 2a). The absolute PL quantum yield (QY) of the PBMSi films at room temperature was found to be around 15% ( $\pm 5\%$ ) depending

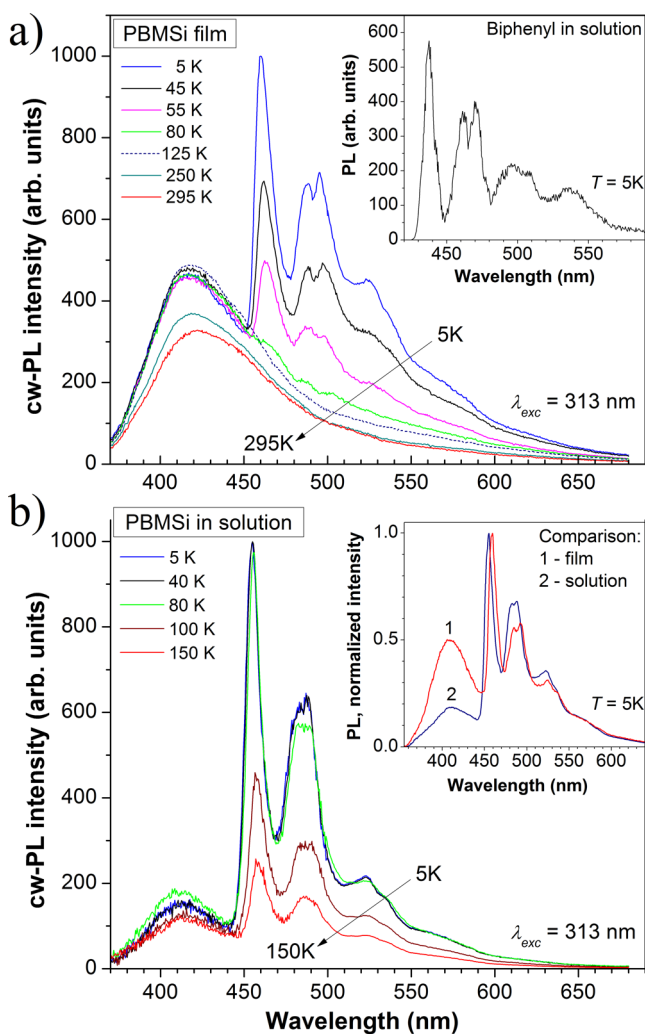


**Figure 2.** (a) Steady-state PL spectra of a 10 μm PBMSi film measured at various temperatures with the excitation at  $\lambda_{\text{exc}} = 313$  nm. The inset shows the steady-state phosphorescence spectra of biphenyl molecules in solution. (b) Steady-state PL spectra of PBMSi in frozen diluted solution in THF measured at various temperatures. The inset shows normalized cw-PL spectra from a 1 μm PBMSi film (curve 1) and from a frozen diluted solution of PBMSi ( $c = 0.01$  wt %) in THF (curve 2).

on the sample, and it increased almost 2-fold upon lowering the temperature to 5 K. An estimated QY for the structured narrow component of the spectrum in PBMSi films was  $\Phi \approx 15\%$ .

The structured spectrum of PBMSi has a fine structure practically identical with that of the phosphorescence spectrum of biphenyl molecules shown in the inset in Figure 2a, albeit it is red-shifted by about  $\sim 1100$   $\text{cm}^{-1}$  with respect to that of biphenyl molecules. Such a bathochromic shift is quite expected owing to the biphenyl groups in PBMSi attached covalently to the polymer main chain. A similar effect is well-known for organic systems, e.g., for poly(vinylcarbazole): due to carbazole pendant groups, its phosphorescence spectrum manifests a bathochromic shift with respect to that of carbazole molecules by  $\Delta\nu = 970$   $\text{cm}^{-1}$  at 5 K.<sup>40</sup>

cw-PL spectra of PBMSi measured in diluted frozen solution under similar excitation conditions are shown in Figure 2b. The inset compares the normalized cw-PL spectra of a PBMSi film (curve 1) and a frozen diluted solution of PBMSi in THF measured at 5 K (curve 2). The PL spectra of the matrix-isolated PBMSi in the frozen solution are basically similar to

that of the PBMSi film, although the structured narrow spectral component is relatively stronger in solution and is readily detectable at temperatures as high as 150 K, before THF starts to melt. These spectra can be observed under excitation at 313 and 365 nm, but no emission from the PBMSi film or frozen solution can be found under the excitation at  $\lambda_{\text{exc}} = 405$  or 436 nm, which confirms complete lack of absorbance in this spectral region.

**Time-Resolved Prompt Fluorescence.** The dynamics of the prompt fluorescence in PBMSi studied by the ultrafast spectroscopy technique is presented in Figure 3. These measurements have revealed two different bands in the fluorescence spectra. A new narrow emission band at 364 nm (3.41 eV) is observed within just several picoseconds after the laser pulse excitation. It decays extremely fast with a lifetime of  $\sim 2.4$  ps (Figure 3b), and therefore, its contribution to the cw-PL spectra is negligible, which probably explains why it has never been reported before. On the other hand, the 415 nm broad band decays much slower, featuring double-exponential kinetics with lifetimes of 1.2 and 2.4 ns at 15 K (not shown). The observed decay time proves the fluorescent character of the 415 nm emission band. Similar results were observed also for PBMSi in the solid films. The spectral position of the 364 nm emission band in PBMSi (Figure 3c) coincides well with the exciton-type PL band typically observed in other poly(silylene)s, such as poly(methylphenylsilylene) (PMPSi).<sup>38,39</sup> Therefore, we conjecture that the PL peak at 364 nm is also of excitonic nature related to the  $\text{Si}^*-\text{Si}$  transition in the PBMSi backbone, although its extremely short lifetime is caused by a very fast relaxation to a lower lying state. One can note a slight bathochromic shift of the 415 nm band to  $\sim 423$  nm (Figure 3a,c) observed in the PBMSi solution within tens of picoseconds at room temperature, which could be rationalized in terms of solvation that is quite typical for organic materials in solutions on such time scales.<sup>41</sup> It should be noted that no structured narrow component at 460 nm (cf. Figure 2) was observed at low temperatures in our time-resolved fluorescent measurements up to 10 ns after the excitation, which implies that its radiative decay rate is much slower.

**Time-Gated Delayed Emission Studies.** To gain insight into the origins of the structured spectral component observed in the cw-PL spectra at low temperature (cf. Figure 2), delayed emission in the PBMSi polymer was measured using the time-gated detection technique with nanosecond time resolution, which enabled detection at much longer time delays. Figure 4 presents the delayed emission spectra detected from a frozen diluted solution of PBMSi ( $T = 80$  K) at various delay times ranging from 70 ns to 10 ms (the delayed emission was reliably detectable up to the largest delay time of the registration system, equal to 25 ms).

The data presented in Figure 4 prove unambiguously the existence of *two different spectral components* in delayed emission spectra of PBMSi, namely, a broad structureless band and a red-shifted well-structured narrow spectral component with the main peak at 460 nm. These spectral components feature *very different decay times*.

The delayed emission at the shortest delay time of 70 ns is completely dominated by the broad structureless band (upper curve in Figure 4). This band decays during several hundred microseconds and is virtually identical to the broad structureless band observed in the prompt fluorescence (Figure 3b) and cw-PL spectra (Figure 2). Therefore, it can be assigned

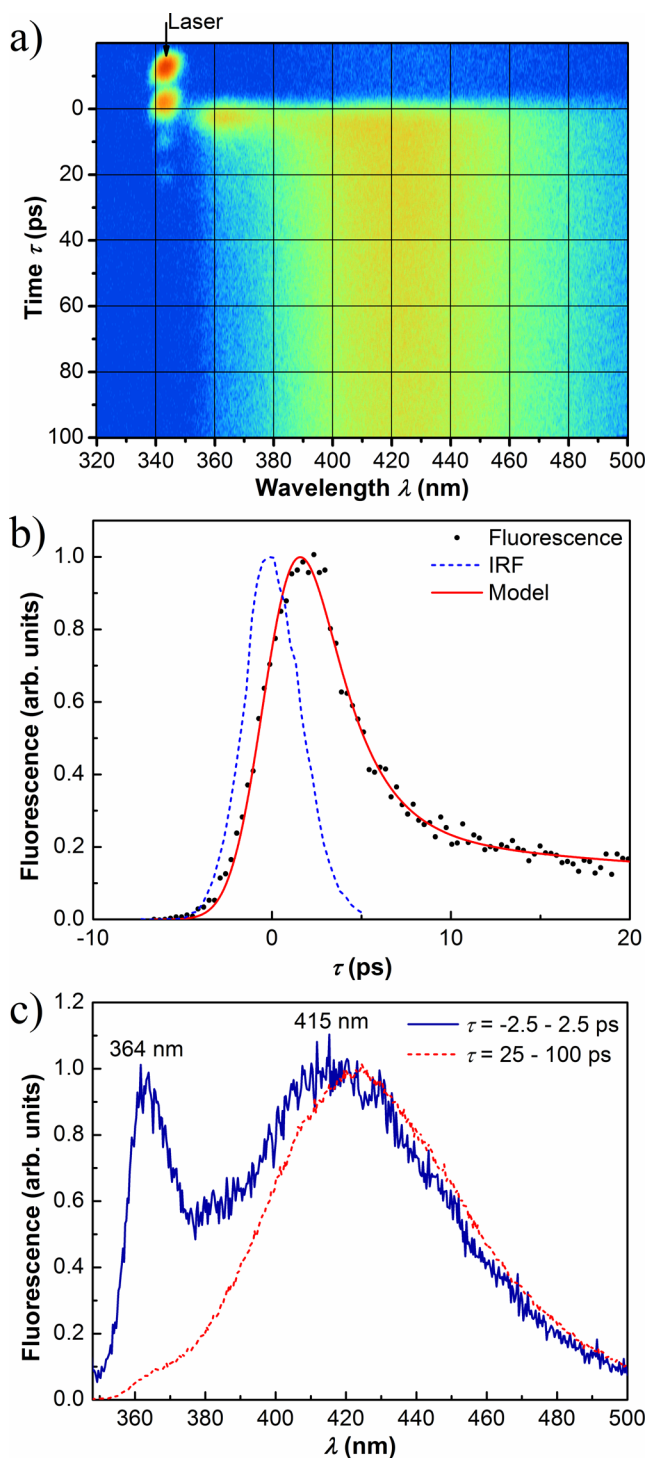


**Figure 3.** (a) Time evolution of prompt fluorescence of PBMSi in toluene solution, measured at room temperature with a streak camera and using sub-100 fs pulses at 343 nm. Signals at 343 nm (arrow) are due to laser light scattering from the cuvette walls. (b) Kinetics of the 364 nm fluorescent band (symbols), instrument response function (IRF) (dashed line), and convolution of a two-exponential decay with the IRF (solid line) fitted to the experimental data. The longer lived decay component is due to spectral overlap with a slower decaying broad spectral band at 415 nm. The obtained decay time of the 364 nm band emission (the shorter lived component) is 2.36 ps. (c) Normalized fluorescence spectra obtained immediately after excitation (blue) and at later times (red).

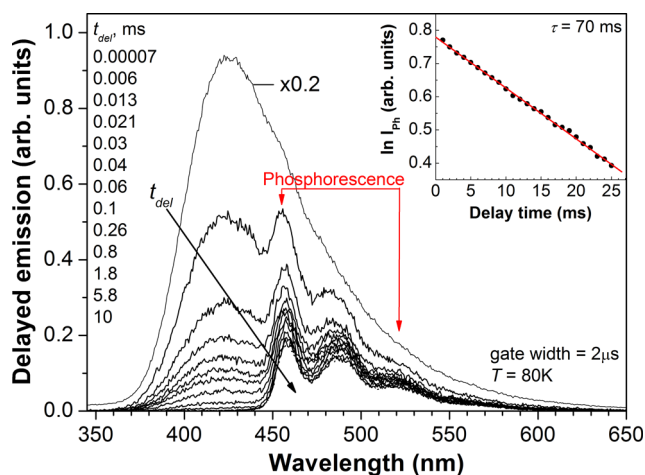


**Figure 4.** Delayed PL spectra of frozen diluted PBMSi solution ( $c = 0.01$  wt %,  $T = 80$  K) at different delay times (shown in the figure) under excitation with  $\lambda_{\text{exc}} = 337$  nm. The time gate width was  $2 \mu\text{s}$ . The upper (70 ns) curve was reduced by a factor of 5. The inset shows time decay kinetics of the spectrally integrated Ph emission component measured in frozen PBMSi solution ( $c = 0.01$  wt %) at 80 K under excitation with  $\lambda_{\text{exc}} = 337$  nm.

to the delayed fluorescence (DF) of PBMSi (its origin will be discussed below).

The second, much slower decaying structured component in the delayed PL spectra in the range of 450–550 nm can only be seen at delay times as large as tens of microseconds, and its contribution to the total delayed emission relatively increases with increasing delay time (Figure 4). This slow decaying spectral component shows all the generic signatures of Ph, principally similar to that previously found in other conjugated polymers, such as MeLPPP,<sup>8,42</sup> ladder-type poly(*p*-phenylene-carbazole) (LPPPC),<sup>43</sup> and polyfluorenes.<sup>44,45</sup> Therefore, it is here assigned to the intrinsic phosphorescence from the  $T_1$  state in pristine PBMSi with a 0–0 transition at 460 nm (2.7 eV) followed by vibronic replicas. Ph completely dominates the delayed emission spectra of the frozen diluted solution of PBMSi at delay times larger than 1 ms (Figure 4). This Ph emission decays monoexponentially, featuring a lifetime  $\tau \approx 70$  ms (see the inset in Figure 4). Such a value of the lifetime is rather typical for Ph of organic semiconductors devoid of heavy atoms, and the monoexponential nature of the decay implies a negligible triplet quenching. In contrast to a solid film, triplet quenching is quite expected to be hindered in a frozen diluted solution due to significantly reduced interchain energy transfer. In the latter case the triplet transport is restricted by migration along separate polymer chains only; therefore, the rarely incorporated quenching centers can hardly be accessible, and monomolecular decay dominates. This has been well documented for  $\pi$ -conjugated polymers.<sup>3,42</sup> In contrast to the other conjugated polymers, the observed Ph in PBMSi is so strong that it can be readily observable even in cw-PL spectra of the PBMSi solid films (Figure 2) for which Ph quenching is expected to be severe because of triplet migration.

The relative intensities of DF and Ph spectral components in the delayed emission spectra of PBMSi depend substantially on the excitation intensity. Figure 5 shows normalized delayed emission spectra measured in the PBMSi solution at 80 K under identical experimental conditions but at high ( $I_{\text{exc}} = 68 \mu\text{J}/(\text{cm}^2 \text{ pulse})$ ) (curve 1) and low ( $I_{\text{exc}} = 2.15 \mu\text{J}/(\text{cm}^2 \text{ pulse})$ ) (curve 2) excitation intensities. The DF component dominates

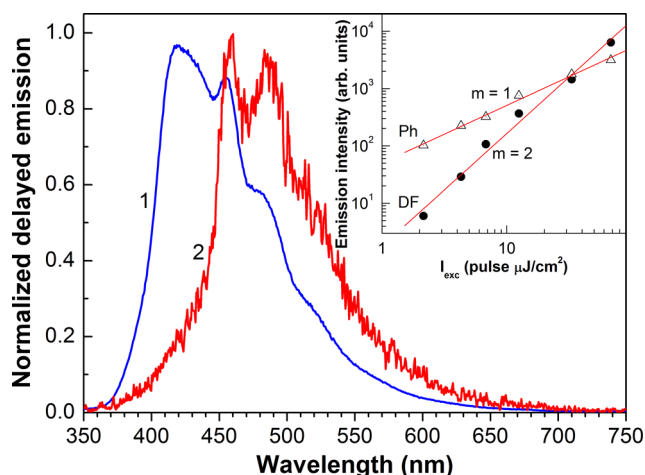


**Figure 5.** Normalized delayed emission spectra of PBMSi in frozen solution ( $T = 80$  K) measured at different laser power intensities: 68 and 2.15  $\mu\text{J}/(\text{cm}^2 \text{ pulse})$  (curves 1 and 2, respectively). Spectra were measured with a delay time of 70 ns and a gate width of 30  $\mu\text{s}$ . The inset shows the dependence of the Ph (triangles) and DF (full circles) intensities of frozen PBMSi solution on the laser excitation intensity ranging from 2.15 to 68  $\mu\text{J}/(\text{cm}^2 \text{ pulse})$ .

the emission spectrum when the polymer is excited at high pumping intensity, while its relative intensity decreases drastically at low intensities of the excitation laser pulses. This unambiguously suggests different excitation mechanisms for the above spectral components. The inset in Figure 5 presents the log–log excitation intensity dependences of the spectrally integrated DF and Ph emission intensities of PBMSi in the frozen solution at 80 K. The Ph intensity varies approximately linearly with the pump intensity within the range of the excitation intensity under consideration (triangles), which agrees with the notion of intersystem crossing being the most probable mechanism for population of the triplet state. The DF (full circles) exhibits a quadratic intensity dependence ( $I_{\text{DF}} \approx I_{\text{exc}}^m$ , where  $m = 2$ ); hence, one could conclude that DF is caused by triplet–triplet annihilation ( $T_1 + T_1 \rightarrow S^* + S_0$ ).<sup>3,45</sup> A similar mechanism of DF was established before for polyfluorene conjugated polymers.<sup>45</sup>

**Triplet Energy Transfer in PBMSi Films.** It is well-known that phosphorescence intensity can be strongly affected by doping of a host polymer film with triplet-sensitizing or triplet-quenching molecules.<sup>16</sup> Such experiments can provide clear proof of the triplet nature of the observed emission and evidence of the triplet energy transfer occurring in the films. Naphthalene ( $\text{C}_{10}\text{H}_8$ ) is expected to be a good triplet quencher for PBMSi because (1) the lowest singlet state of naphthalene in a frozen solution,  $S_1 = 3.93$  eV (315 nm), is considerably higher than that of PBMSi, while (2) the triplet state of naphthalene,  $T_1 = 2.63$  eV (471 nm), is below the triplet state of the host polymer (2.7 eV). Figure 6a shows the normalized cw-PL spectra measured at  $T = 5$  K in both the neat PBMSi film (curve 1) and the PBMSi film doped with naphthalene ( $c = 10$  wt %) (curve 2). As expected, the intrinsic structured Ph spectrum of the PBMSi polymer was almost completely quenched by naphthalene dopant molecules (Figure 6, curve 2), and at the same time, the characteristic Ph spectrum ( $T_1 \pi\text{-}\pi^* \rightarrow S_0$ ) of naphthalene<sup>46</sup> with the 0–0 transition at about 474 nm followed by vibronic replicas appeared.

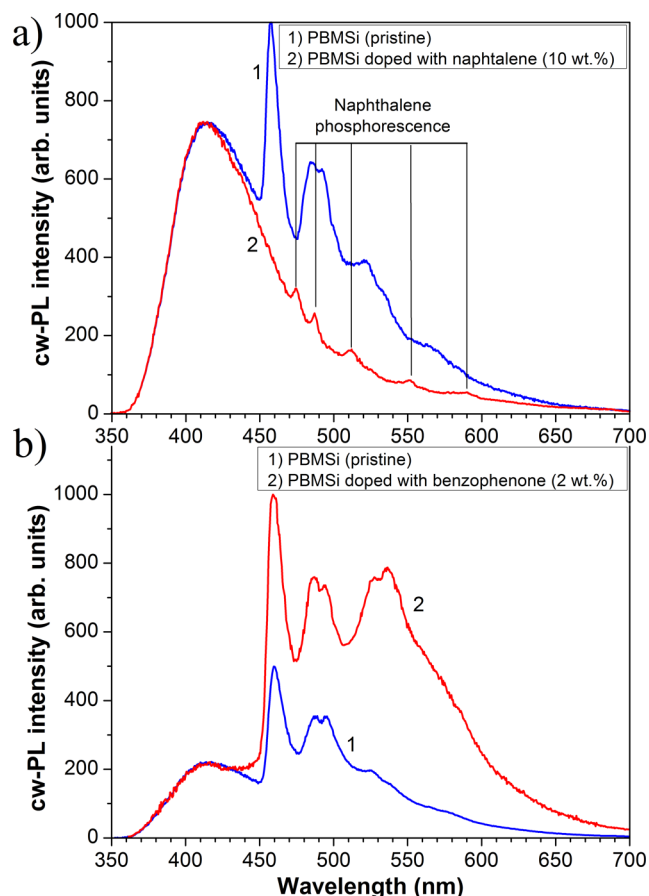


**Figure 6.** Comparison of normalized cw-PL spectra of the neat PBMSi film (curve 1) with that of the PBMSi film doped ( $c = 10$  wt %) with naphthalene (a, curve 2) and the PBMSi film doped ( $c = 2$  wt %) with benzophenone (b, curve 2). All spectra were measured under excitation with  $\lambda_{\text{exc}} = 313$  nm at  $T = 5$  K.

Benzophenone, which exhibits an ISC process with an efficiency of nearly 100%,<sup>47</sup> could act as a sort of sensitizer of the host polymer phosphorescence because the  $S_1$  state of benzophenone is at 3.29 eV ( $\sim 377$  nm), i.e., below that of PBMSi, and the benzophenone triplet is at 3.01 eV (412 nm),<sup>46</sup> i.e., 0.31 eV above the  $T_1$  state of the PBMSi host. Figure 6b compares the normalized cw-PL spectrum of the neat PBMSi film (curve 1) and the spectrum of the PBMSi film doped with benzophenone ( $c = 2$  wt %) (curve 2) measured at 5 K. A considerable relative enhancement of the PBMSi Ph spectral component is obvious without any traces of the benzophenone phosphorescence. This implies an efficient triplet energy transfer from guest benzophenone molecules to the polymer host, which is ensured by the so-called “ping-pong” effect<sup>48</sup> when the singlet energy is first transferred from the host polymer to guest molecules and then, after intersystem crossing from the  $S_1$  state to the  $T_1$  state of the benzophenone molecule, the guest triplets are transferred back to the host, thus increasing the concentration of triplets in the PBMSi polymer.

The observations of the triplet energy transfer processes shown in Figure 6 prove straightforwardly the triplet origin of the structured narrow spectral component of the PBMSi polymers and imply efficient triplet exciton migration in these polymers even at 5 K. We have also observed efficient triplet energy transfer from the PBMSi polymer host to guest organometallic complexes and white light emission from

PBMSi doped with suitable materials (see section 4 of the Supporting Information).

## COMPUTATION RESULTS

To clarify the nature of the excited states in PBMSi, electronic excitations in a model system containing the principal moieties of the polymer were studied by means of quantum-mechanical computations. The model system was formed by placing the biphenyl-4-ylmethylsilane monomer in the middle of a dimethylsilane oligomer chain (MSi15-BP). The length of the oligosilane chain was initially varied to achieve the absorption energies comparable with the experimental data. The chain of 15 repeat units was chosen for the best trade-off between accuracy and computational complexity. The structure of the resulting model system, the MSi15-BP oligomer, is shown in Figure 7.

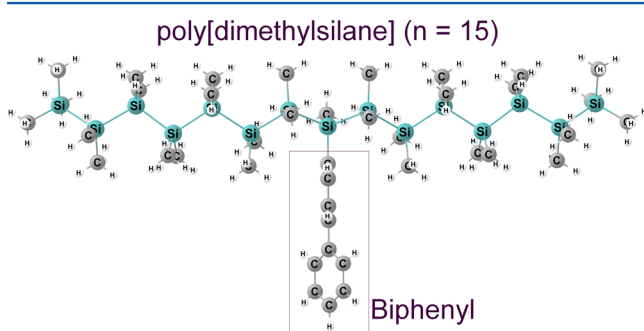


**Figure 7.** Molecular structure of the 4-[pentadecakis-(dimethylsilylene)]biphenyl (MSi15-BP) oligomer in the ground electronic state calculated using the DFT approach.

The properties of the singlet and triplet electronic excitations of the MSi15-BP oligomer calculated by TD-DFT for the oligomer structure optimized in the ground electronic state (the  $S_0$  conformer in Figure 8) are summarized in Table 1, and the corresponding molecular orbitals participating in the lowest lying excitations are presented in the Supporting Information

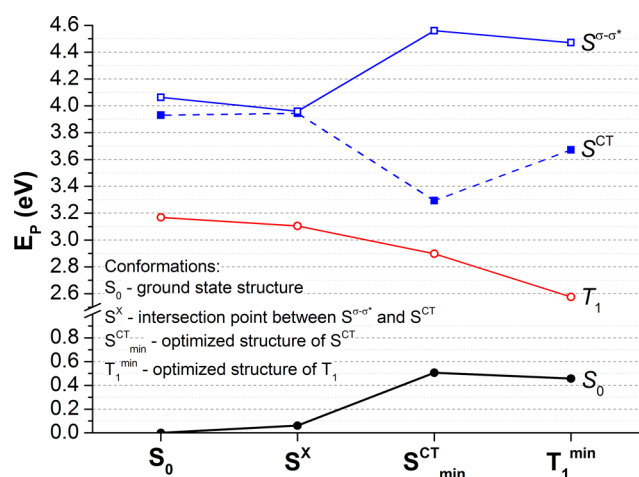


**Figure 8.** Potential energy values ( $E_p$ ) of the ground and low-lying excited states of the MSi15-BP oligomer for the different structural conformations of the compound, based on the TD-DFT calculations.

The  $S^{\sigma-\sigma^*}$  state does not have an explicit minimum in the vicinity of the vertical absorption, but rather it has an intersection point with the  $S^{\text{CT}}$  state, enabling fast internal conversion between the two states.

**Table 1. Properties<sup>a</sup> of the Excited Electronic States of the MSi15-BP Oligomer in the Ground-State Geometry Based on the TD-DFT Calculations and Obtained by the GMC-QDPT Calculations (in Parentheses)**

state	$E_{\text{exc}}$ eV	$f_{\text{osc}}$	transition <sup>b</sup>	weight
1: $T_1 \pi-\pi^*$	3.17 (3.23)		3-1'	0.522
2: $T_2 \sigma-\sigma^*$	3.73 (4.46)		1-2'	0.684
3: $T_3^{\text{CT}}$	3.81 (5.69)		1-1'	0.363
4: $S^{\text{CT}}$	3.93 (4.84)	0.113 (0.405)	1-1'	0.693
5: $T_4^{\text{CT}}$	4.02 (5.92)		1-1'	0.500
...				
7: $S^{\sigma-\sigma^*}$	4.06 (5.53)	2.510 (1.568)	1-2'	0.679
...				
18: $S^{\pi-\pi^*}$	4.68 (6.42)	0.281 (0.434)	3-1'	0.557

<sup>a</sup>The table contains the following properties: excitation energies ( $E_{\text{exc}}$ ), oscillator strengths ( $f_{\text{osc}}$ ), principal one-electron transition corresponding to the current excited state and its relative contribution. <sup>b</sup>In the "transition" column, occupied molecular orbitals are denoted as 1, 2, 3, ..., starting from the HOMO, and virtual molecular orbitals are denoted as 1', 2', 3', ..., starting from the LUMO.

(Figure S1). The essential findings of the above TD-DFT calculations for the  $S_0$  conformer are the following:

(1) The lowest singlet excited state ( $S^{\text{CT}} = 3.93$  eV) was found to contain a dominant charge-transfer character corresponding to the Si  $\rightarrow$  BP transition. The oscillator strength for the  $S_0-S^{\text{CT}}$  transition is small, but nonvanishing.

(2) The second calculated singlet excited state has a clear intrachain character and corresponds to a  $\sigma-\sigma^*$ -type transition in the Si chain ( $S^{\sigma-\sigma^*} = 4.06$  eV). It is optically active and, therefore, can be attributed to the first (main) band in the absorption spectrum measured in the PBMSi polymer. The optically allowed singlet  $\pi-\pi^*$  transitions in the BP moiety are of considerably higher energy ( $>4.68$  eV).

(3) Several low-lying triplet states were defined from calculations, and three of them were found below the lowest singlet state. The lowest triplet state of the MSi15-BP oligomer ( $T_1^{\pi-\pi^*} = 3.17$  eV) is of  $\pi-\pi^*$  nature due to the BP moiety, in agreement with the experimental observations.

(4) Interestingly, a triplet state of the CT character ( $T_3^{\text{CT}} = 3.81$  eV) was found slightly below the lowest singlet CT state ( $S^{\text{CT}} = 3.93$  eV), implying a singlet-triplet splitting of 0.12 eV, which is much smaller than that for intrachain excitations. In addition, one more triplet state of CT character ( $T_4^{\text{CT}} = 4.02$  eV) was found slightly above the lowest singlet ( $S^{\text{CT}}$ ) state.

(5) A triplet on-chain excitation of the Si chain itself ( $T_2^{\sigma-\sigma^*} = 3.73$  eV) was found to be of  $\sigma-\sigma^*$  character, and its energy is located between those of the above-mentioned  $T_1^{\pi-\pi^*}$  and  $T_3^{\text{CT}}$  states.

Generally, the calculated electronic transitions are shifted to higher energies compared to the experimentally obtained values, mainly because of the limitations of the employed basis set and the limited oligomer length. However, the mutual arrangement of the calculated energy levels agrees with the experimental data reasonably well. The calculations have proved a large singlet-triplet splitting between the  $S^{\sigma-\sigma^*}$  and  $T_1^{\pi-\pi^*}$  states of the MSi15-BP oligomer that is expected for conjugated polymers and is comparable with the experimental observations.

An important result of the TD-DFT calculations (Table 1) is the fact that the singlet CT state ( $S^{CT}$ ) is predicted to be below the optically allowed state  $S^{\sigma-\sigma^*}$ . This qualitatively agrees with the experimentally measured fluorescence spectra of PBMSi (see Figure 3c). The calculated bathochromic shift of 0.13 eV with respect to the  $S^{\sigma-\sigma^*}$  state at the initial geometry is expected to be significantly underestimated because an additional molecular relaxation in the charge-separated system (which should result in lowering of the  $S^{CT}$  energy) is not accounted for in this case. Indeed, after the optimization of the geometric parameters of the  $S^{CT}$  state, its transition energy was found to be equal to 2.79 eV (Figure 8). This corresponds to the bathochromic shift of up to 1.22 eV ( $4.01 - 2.79 = 1.22$ ), which already overestimates the experimental value of 0.67 eV ( $3.65 - 2.98 = 0.67$ ). In reality, the structure of the polymer during  $S^{CT}$  emission would not be fully relaxed, corresponding to the less shifted values. The presence of the low-lying CT state in this material is also supported by consideration of the shapes of the molecular orbitals in MSi15-BP (especially of the HOMO in Figures S1 and S2 of the Supporting Information), which indicate a partial overlap between the  $\pi$ -system of the biphenyl group and the  $\sigma$ -conjugated chain of polysilylene that would facilitate an intramolecular charge transfer between them.

The structure rearrangements taking place in different excited states lead to changes of the state energies. The energy of the relaxed  $S^{CT}$  state drops significantly below that of the  $S^{\sigma-\sigma^*}$  state. The molecular relaxation in the  $S^{\sigma-\sigma^*}$  state leads to the nearby intersection point ( $S^X$ ) between the  $S^{\sigma-\sigma^*}$  and  $S^{CT}$  states that is only 0.17 eV lower than the initial  $S^{\sigma-\sigma^*}$  state energy (Figure 8). This result shows the possibility of nonradiative internal conversion from the  $S^{\sigma-\sigma^*}$  state to the  $S^{CT}$  state. Moreover, the change of the geometric parameters of the MSi15-BP compound during this process is negligible: Si–Si bond lengths are lengthened by 0.002 Å and Si–Si–Si valence angles are enlarged by  $0.2^\circ$  only. This additionally supports the possibility of a fast  $S^{\sigma-\sigma^*} \rightarrow S^{CT}$  conversion process. The subsequent structural relaxation of the  $S^{CT}$  or  $T_1^{\pi-\pi^*}$  state involves more pronounced structural changes that result in an increase of the ground-state energy by about 0.5 eV. Corresponding transition energy values for the structurally optimized  $S^{CT}$  and  $T_1^{\pi-\pi^*}$  states are 2.79 eV (445 nm) and 2.12 eV (585 nm), respectively. The difference between the measured and calculated Ph energy values can be rationalized as arising from two main causes. First, taking into account the environment of the experimentally studied PBMSi polymer, it is very likely that the observed photoemission takes place before the structure of the polymer in the excited state is fully relaxed. Second, the reorganization energy of the polymer segment related to its structural relaxation is known to decrease with increasing size of the conjugated system; therefore, the relaxation may have been overestimated during the calculations by using a model compound of a limited length.

## DISCUSSION

A remarkable finding of this study is that the  $\sigma$ -conjugated polymer PBMSi shows unusually strong phosphorescence (in comparison with other conjugated polymers), which is easily detectable even in steady-state PL spectra and dominates these

spectra at low temperatures. The observed phosphorescence is an *intrinsic emission* of the polymer since it significantly increases in frozen diluted solutions as compared to solid films (see the inset in Figure 2b), which excludes the role of extrinsic phosphorescent impurities. This conclusion is also supported by the triplet energy transfer experiments in PBMSi films doped with triplet-sensitizing or triplet-quenching molecules (Figure 6). Temperature quenching of the Ph intensity observed in the PBMSi films can readily be explained by a diffusion-controlled quenching of triplet excitons by some sort of accidental quenching centers such as molecular oxygen, which is enhanced with increasing temperature due to the thermally activated character of exciton diffusivity in disordered solids. It has to be noted that polymer films used in this study were prepared without any special protection to avoid oxygen during film deposition and were exposed to air prior to the measurements, so the presence of molecular oxygen is very probable in the studied films.

As follows from Figure 2a and the inset to this figure, the observed Ph of PBMSi is due to the radiative decay of triplets on the biphenyl side group, which has also been corroborated by both TD-DFT and ab initio GMC-QDPT calculations (cf. Table 1). This unambiguously suggests a strongly *enhanced* ISC in this polymer, which eventually enables an efficient conversion of primary excited singlets of the  $\sigma$ -conjugated silicon main chain of the polymer into triplets of the  $\pi$ -conjugated biphenyl side group. Biphenyl is well-known as a good phosphorescent material itself;<sup>49</sup> however, in our experiment photoexcitation energies have been far lower than the absorption band of the biphenyl side group. The biphenyl group absorbs at around 258 nm (cf. Figure 1), while the Ph emission of PBMSi is observable under excitation with 313, 337, and even 366 nm, i.e., at the excitation within the tail of the absorption spectrum of the polymer. This implies that in our experiment the  $T_1^{\pi-\pi^*}$  state of the biphenyl moiety of PBMSi is populated *indirectly* primarily via the generated singlet  $S^{\sigma-\sigma^*}$  state of the  $\sigma$ -conjugated polymer backbone and not via the singlet state on the biphenyl group itself. Remarkably, the observed intrinsic Ph in the PBMSi polymer (which does not contain any heavy atoms) features a quantum yield of about 15% in solid films that is quite comparable to that of Pt-containing conjugated polymers<sup>5–7</sup> or some organometallic complexes.<sup>4</sup> Normally, the phosphorescent quantum yields in both  $\pi$ - and  $\sigma$ -conjugated polymers are 4–5 orders of magnitude smaller.<sup>3,8</sup>

To rationalize the findings, one should consider the excited-state energy structure of this polymer, which clearly plays a key role in the observed phenomena:

(1) The lowest optically allowed singlet excited state of PBMSi, responsible for the longest wavelength absorption band in the near-UV region at 340 nm, is due to the delocalized  $\sigma-\sigma^*$  transition in the Si polymer backbone ( $S^{\sigma-\sigma^*} = 3.65$  eV), which is typical for poly(silylene) polymers, such as PMPSi or poly(dihexylsilylene).<sup>38,39</sup> The latter polymers normally show an intensive cw-PL spectrum with the relatively narrow main band at  $\sim 360$  nm that is the mirror image of the absorption band<sup>38</sup> and is conventionally ascribed to an exciton-type emission of the main polymer Si chain. In contrast, the steady-state PL spectrum of PBMSi features a broad PL band at 416 nm which is strongly bathochromically shifted (by 0.67 eV) with respect to the lowest energy absorption band, suggesting that its nature is different from that of the conventional singlet

exciton in poly(silylene)s. It is remarkable that it was possible to detect the narrow emission band at 364 nm (3.41 eV) in PBMSi with an ultrafast PL spectroscopy technique (Figure 3). The position of this band is almost identical to that of the exciton PL band observed in PMPSi; therefore, we ascribe the 364 nm PL band to the exciton emission. Thus, conventional excitonic state levels related to the main Si chain are basically similar for both PBMSi and PMPSi polymers.

(2) The extremely fast (within a few picoseconds) decay of the above-mentioned exciton fluorescence band at 364 nm (Figure 3) implies a very fast nonradiative energy relaxation to a lower energy state. The quantum-mechanical calculations confirm the existence of a singlet state of charge-transfer character ( $S^{\text{CT}}$ ) below the excitonic singlet  $S^{\sigma-\sigma^*}$  state. The intersection point between the  $S^{\sigma-\sigma^*}$  and  $S^{\text{CT}}$  states determined by the TD-DFT calculations (Figure 8) can facilitate fast internal conversion between these states. The  $S^{\text{CT}}$  state originates from intramolecular electron transfer from the excited  $\sigma$ -conjugated Si chain to the biphenyl side group as proven by the calculated shapes of the molecular orbitals (Figures S1 and S2 in the Supporting Information). The Si chain in this case exhibits electron donation properties, while the biphenyl moiety acts as an electron acceptor. In terms of molecular spectroscopy, this  $S^{\text{CT}}$  state can be considered as a kind of intramolecular “excimer-type” state, and it is responsible for the broad band at 416 nm in the cw-PL spectra of this polymer. The GMC-QDPT calculations yield a radiative lifetime of 0.89 ns that agrees reasonably well with the observed 1.2 ns lifetime measured in PBMSi for the 416 nm PL band. The bathochromic shift (0.67 eV) of this band with respect to the absorption as well as the exciton band is quite typical for the excimer-type emission in organic materials. The TD-DFT calculations also predict that the oscillator strength of the exciton transition ( $S_0 \rightarrow S^{\sigma-\sigma^*}$ ),  $f_{\text{osc}} = 2.51$ , is much larger than  $f_{\text{osc}} = 0.113$  of the CT state ( $S_0 \rightarrow S^{\text{CT}}$ ) (Table 1); this agrees with the experimental observation that the absorption of PBMSi is dominated by the  $\sigma-\sigma^*$  transition within the main polymer chain. Thus, the above arguments prove the existence of the intramolecular CT state in PBMSi below the conventional exciton state.

(3) Both TD-DFT and ab initio GMC-QDPT calculations confirm that the lowest triplet state in PBMSi is  $T_1^{\pi-\pi^*}$  of the biphenyl group. The calculations yield other triplet states of different character, e.g., the triplet state of the  $\sigma$ -conjugated main Si chain of the PBMSi ( $T_2^{\sigma-\sigma^*}$ ) located above  $T_1^{\pi-\pi^*}$  (Table 1). This agrees perfectly with the experimental observation of a strong Ph due to the biphenyl moiety (Figure 2), implying that there are no other intrinsic triplet states below that would otherwise be able to quench this Ph emission.

(4) Importantly, the TD-DFT calculations yield the triplet state of CT character ( $T_3^{\text{CT}} = 3.81$  eV) to be located slightly below  $S^{\text{CT}} = 3.93$  eV (Table 1), implying a very small singlet–triplet splitting (0.12 eV) for the intramolecular charge-transfer excitations in this material. We should underline that observed positive S–T splitting ( $\Delta E_{\text{ST}} > 0$ ) is a nontrivial result because recent quantum chemical calculations have demonstrated<sup>50</sup> that the situation can be the opposite for *intermolecular* CT states where singlet CT states often lie energetically below the triplet CT states; i.e., the S–T splitting is negative ( $\Delta E_{\text{ST}} < 0$ ). On the other hand, it has been reported by Difley et al.<sup>50</sup> that  $\Delta E_{\text{ST}}$  of organic dyes and oligomers depends sensitively on both the

material and the relative orientation of the donor–acceptor pair. The observed splitting is much smaller than any other S–T gap in this system and considerably smaller than the conventional value of  $\sim 0.7$  eV of neutral on-chain excitations in  $\pi$ -conjugated polymers.<sup>16</sup> It should be mentioned that a considerably reduced S–T splitting is quite expected for interchain electron–hole (e–h) pairs in organic materials.<sup>12</sup> The triplet polaron-pair state was found to be 6 meV below that of the corresponding singlet for the MeLPPP polymer using thermally stimulated luminescence.<sup>17</sup> This is because of the reduced exchange interaction in e–h pairs,<sup>12,17,51</sup> which results in a closer energy separation of the singlet and triplet state energy levels in the e–h pair manifold compared to the exciton manifold. The proximity of CT states is very favorable for an enhanced intersystem crossing rate.<sup>12</sup> It should be noted that although the CT state in PBMSi is of *intramolecular* nature, the underlying physical mechanisms should basically be the same as for *intermolecular* CT states.

The considerations presented above demonstrate that the experimental data and the results of quantum-mechanical calculations are consistent in terms of the excited state level arrangement and the order of relaxation processes. This allows us to suggest the following scenario for the enhanced ISC in PBMSi polymers. Figure 9 shows the energy diagram calculated

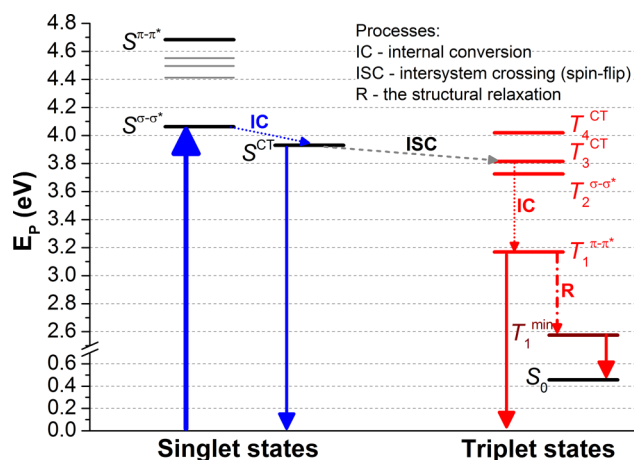


**Figure 9.** Electronic excitations and relaxation pathways of MSi15-BP based on the TD-DFT calculations.

by TD-DFT and possible relaxation pathways. The ISC can only occur from the  $S^{\text{CT}}$  state since the primary singlet photoexcitation  $S^{\sigma-\sigma^*}$  undergoes very fast nonradiative internal conversion to the lower lying  $S^{\text{CT}}$  state with a rate as high as  $\sim 0.5$  ps<sup>-1</sup>. The experimental lifetime of the  $S^{\text{CT}}$  state itself is  $\tau \approx 1$  ns (a longer lived component with  $\tau \approx 2.4$  ns was also observed). This value is somewhat larger than the typical lifetime on the order of hundreds of picoseconds reported for neutral singlet on-chain excitation in poly(silylene)s such as PMPSi,<sup>52</sup> and therefore, this should facilitate the ISC. However, the observed longer lifetime of the  $S^{\text{CT}}$  state does not necessarily lead to increased phosphorescence in similar systems; for example, no phosphorescence has been observed from poly(di-*n*-hexylsilylene), a compound featuring a fluorescence lifetime comparable to that of PBMSi. The ISC from the singlet  $S^{\text{CT}}$  state occurs mostly to the triplet  $T_3^{\text{CT}}$  state (Figure 9) because the S–T splitting is positive, and the rate of this ISC is enhanced due to weak exchange interaction of a

spatially separated electron and hole in the CT state, resulting in a *considerably smaller* singlet–triplet energy splitting (0.12 eV) compared to that for neutral excitons. Since the quantum efficiency of the intrinsic phosphorescence in PBMSi was found to be around  $\Phi \approx 15\%$ , this number sets the low limit of the ISE in this polymer, which is at least 1–2 orders higher than in conventional conjugated polymers. Direct  $S^{\text{CT}} \rightarrow T_1^{\pi-\pi^*}$  transition may also be possible; however, its rate is expected to be considerably smaller both due to much larger energy spacing between these levels and due to the fact that the  $\sigma$ -orbital of  $S^{\text{CT}}$  is partially mixed with the  $\pi$ -system of biphenyl, which would diminish the vibrational overlap.<sup>53</sup> Thus, the  $S^{\text{CT}} \rightarrow T_3^{\text{CT}}$  channel dominates the ISC process and determines its high efficiency in PBMSi. Finally, the  $T_3^{\text{CT}}$  excited state decays nonradiatively to the lower lying triplet states of PBMSi (Figure 9) as this is a spin-allowed process and back electron transfer (recombination) can produce triplet states of both the Si chain ( $T_2^{\sigma-\sigma^*}$ ) and the BP moiety ( $T_1^{\pi-\pi^*}$ ). The  $T_1^{\pi-\pi^*}$  state will eventually be populated due to its lower energy (Table 1).

A somewhat similar scenario for strong enhancement of the ISC has recently been suggested for donor–acceptor CuPC:PCBM blends<sup>12</sup> where the ISC rate was found to be very high due to reduced S–T energy splitting in the photogenerated *intermolecular* charge-carrier pairs. This issue is currently of considerable interest for organic photovoltaics where ISC is expected to be substantially faster than the standard intersystem crossing in conjugated polymers. PBMSi has a very small intramolecular  $S^{\text{CT}}-T^{\text{CT}}$  gap and possesses the lowest triplet state  $T_1^{\pi-\pi^*}$  below the CT state, which perfectly matches the conditions for e–h pair recombination,<sup>51</sup> even though it involves an intramolecular CT state rather than a donor–acceptor pair, as was the case in the paper by Snedden et al.<sup>12</sup> Thus, we demonstrate the ISC enhancement mechanism realized within a neat conjugated polymer comprising suitable donor ( $\sigma$ -conjugated backbone) and acceptor ( $\pi$ -conjugated side group) moieties. Such findings provide additional insight into the effects of CT states on intersystem crossing and triplet formation.

A small S–T splitting of 0.12 eV might in principle be sufficient for also facilitating an RISC of triplets<sup>18–20</sup> from the  $T_3^{\text{CT}}$  state to singlets at the  $S^{\text{CT}}$  state at high enough temperature and might hence enable a TADF emission in PBMSi. However, because of a quick (spin-allowed) decay of the  $T_3^{\text{CT}}$  state to the lower lying triplet states (Figure 9), the RISC is only likely to occur between  $T_1^{\pi-\pi^*}$  and  $S^{\text{CT}}$  states that are separated more widely (by 0.28 eV). The TADF has been demonstrated for some materials featuring  $\Delta E_{\text{ST}}$  as large as 0.24 eV,<sup>54</sup> but only at temperatures in the region from 300 to 400 K. It might well be possible that similar phenomena occur in PBMSi at high temperatures. However, to establish this, a more detailed investigation using an inert environment (to provide adequate protection against oxygen during sample preparation) would be required.

One should note that the increased ISC rate for conversion of singlets of the polymer chain to triplets of the biphenyl side group seemingly does not lead to a considerable increase of the radiative  $T_1^{\pi-\pi^*} \rightarrow S_0$  transition rate within the biphenyl moiety. This is because the latter process occurs between orbitals of the same  $\pi-\pi^*$  nature, which results in a “normal” Ph lifetime of  $\sim 70$  ms; i.e., this transition remains virtually unaffected. This circumstance manifests an important difference

between the observed increase of the ISC rate in this study and that known from the heavy atom effect. In the latter case, a heavy atom enhances both the population of the triplet state via the  $S^* \rightarrow T_1^*$  transition and its *deactivation* via the  $T_1^* \rightarrow S_0$  transition due to inevitable shortening of the triplet lifetime, which reduces accumulation of triplet excitations in such materials as well as the triplet diffusion length. On the other hand, accumulation of a large concentration of triplets might, in principle, be desirable for some applications, e.g., in systems for noncoherent TTA-UC<sup>13,14</sup> and for creation of a suitable organic phosphorescent material as a laser emitter.<sup>55</sup> The present study can contribute to a new molecular-level engineering approach for strong enhancement of ISC for efficient conversion of primary excited singlets into triplets in conjugated polymers not requiring the heavy atom effect. Finally, it should be mentioned that PBMSi could be a promising active polymer host layer for creation of white-light-emitting OLED devices due to a relatively high intrinsic triplet level and efficient triplet energy transfer, as well as charge-carrier mobility in excess of  $10^{-4}$  cm<sup>2</sup>/(V s), which is fairly large for polymers.<sup>56</sup>

## ■ ASSOCIATED CONTENT

### 📄 Supporting Information

Description of the spectroscopy techniques used during the experiment (section 1), comparison of the results of TD-DFT and GMC-QDPT calculations (section 2), geometries and total energies of the investigated structural conformations of the MSi5-BP compound (Tables S1–S4), molecular orbitals of the compound associated with the lowest lying one-electron transitions (Figures S1 and S2), and spectra of PBMSi films doped with organometallic complexes (section 4). This material is available free of charge via the Internet at <http://pubs.acs.org>.

## ■ AUTHOR INFORMATION

### Corresponding Author

\*E-mail: [kadash@iop.kiev.ua](mailto:kadash@iop.kiev.ua).

### Notes

The authors declare no competing financial interest.

## ■ ACKNOWLEDGMENTS

This research was supported by the European Research Council via Grant No. 320680 (EPOS CRYSTALLI), by the NAS of Ukraine via the program for fundamental research on nanophysics (Project No. 1/13-H-23K), by the collaboration project M/318-2013 of DKNII of Ukraine, by the European Regional Development Fund, and by the Ministry of Education, Youth and Sports of the Czech Republic under the Regional Innovation Centre for Electrical Engineering (RICE), Project No. ED2.2.00/03.0094c. Computations were performed using the resources of the High Performance Computing Center “HPC Saulėtekis” in the Faculty of Physics at Vilnius University. We gratefully acknowledge valuable discussions with Prof. H. Bässler and Dr. Chang-Hwan Kim.

## ■ REFERENCES

- (1) Baldo, M. A.; O'Brien, D. F.; You, Y.; Shoustikov, A.; Silbey, S.; Thompson, M. E.; Forrest, S. R. Highly Efficient Phosphorescent Emission from Organic Electroluminescent Devices. *Nature* **1998**, *395*, 151–154.

- (2) Adachi, C.; Baldo, M. A.; Thompson, M. E.; Forrest, S. R. Nearly 100% Internal Phosphorescence Efficiency in an Organic Light-Emitting Device. *J. Appl. Phys.* **2001**, *90*, 5048–5051.
- (3) Köhler, A.; Bässler, H. Triplet States in Organic Semiconductors. *Mater. Sci. Eng., R* **2009**, *66*, 71–109.
- (4) Lamansky, S.; Djurovich, P.; Murphy, D.; Abdel-Razzaq, F.; Lee, H.-E.; Adachi, C.; Burrows, P. E.; Forrest, S. R.; Thompson, M. E. Highly Phosphorescent Bis-Cyclometalated Iridium Complexes: Synthesis, Photophysical Characterization, and Use in Organic Light Emitting Diodes. *J. Am. Chem. Soc.* **2001**, *123*, 4304–4312.
- (5) Köhler, A.; Wilson, J. S.; Friend, R. H.; Al-Suti, M. K.; Khan, M. S.; Gerhard, A.; Bässler, H. The Singlet–Triplet Energy Gap in Organic and Pt-Containing Phenylene Ethynylene Polymers and Monomers. *J. Chem. Phys.* **2002**, *116*, 9457–9463.
- (6) Wilson, J. S.; Chawdhury, N.; Al-Mandhary, M. R. A.; Younus, M.; Khan, M. S.; Raithby, P. R.; Köhler, A.; Friend, R. H. The Energy Gap Law for Triplet States in Pt-Containing Conjugated Polymers and Monomers. *J. Am. Chem. Soc.* **2001**, *123*, 9412–9417.
- (7) Sudha Devi, L.; Al-Suti, M. K.; Dosche, C.; Khan, M. S.; Friend, R. H.; Köhler, A. Triplet Energy Transfer in Conjugated Polymers. I. Experimental Investigation of a Weakly Disordered Compound. *Phys. Rev. B* **2008**, *78*, 045210.
- (8) Romanovskii, Yu. V.; Gerhard, A.; Schweitzer, B.; Scherf, U.; Personov, R. I.; Bässler, H. Phosphorescence of  $\pi$ -Conjugated Oligomers and Polymers. *Phys. Rev. Lett.* **2000**, *84*, 1027–1030.
- (9) Laquai, F.; Im, C.; Kadashchuk, A.; Bässler, H. Sensitized Intrinsic Phosphorescence from a Poly(phenylene-vinylene) Derivative. *Chem. Phys. Lett.* **2003**, *375*, 286–291.
- (10) Xuan, Y.; Pan, D.; Zhao, N.; Ji, X.; Ma, D. White Electroluminescence from a Poly(N-vinylcarbazole) Layer Doped with CdSe/CdS Core–Shell Quantum Dots. *Nanotechnology* **2006**, *17*, 4966–4969.
- (11) Reineke, S.; Thomschke, M.; Lüssem, B.; Leo, K. White Organic Light-Emitting Diodes: Status and Perspective. *Rev. Mod. Phys.* **2013**, *85*, 1245–1293.
- (12) Snedden, E. W.; Monkman, A. P.; Dias, F. B. Photophysics of the Geminate Polaron-Pair State in Copper Phthalocyanine Organic Photovoltaic Blends: Evidence for Enhanced Intersystem Crossing. *Adv. Mater.* **2013**, *25*, 1930–1938.
- (13) Monguzzi, A.; Tubino, R.; Meinardi, F. Upconversion-Induced Delayed Fluorescence in Multicomponent Organic Systems: Role of Dexter Energy Transfer. *Phys. Rev. B* **2008**, *77*, 155122.
- (14) Nattestad, A.; Cheng, Y. Y.; MacQueen, R. W.; Schulze, T. F.; Thompson, F. W.; Mozer, A. J.; Fucel, B.; Khoury, T.; Crossley, M. J.; Lips, K.; et al. Dye-Sensitized Solar Cell with Integrated Triplet–Triplet Annihilation Upconversion System. *J. Phys. Chem. Lett.* **2013**, *4*, 2073–2078.
- (15) Webster, S.; Peceli, D.; Hu, H.; Padilha, L. A.; Przhonska, O. V.; Masunov, A. E.; Gerasov, A. O.; Kachkovski, A. D.; Slominsky, Y. L.; Tolmachev, A. I.; et al. Near-Unity Quantum Yields for Intersystem Crossing and Singlet Oxygen Generation in Polymethine-like Molecules: Design and Experimental Realization. *J. Phys. Chem. Lett.* **2010**, *1*, 2354–2360.
- (16) Monkman, A. P.; Burrows, H. D.; Hartwell, L. J.; Horsburgh, L. E.; Hamblett, I.; Navaratnam, S. Triplet Energies of  $\pi$ -Conjugated Polymers. *Phys. Rev. Lett.* **2001**, *86*, 1358–1361.
- (17) Kadashchuk, A.; Vakhnin, A.; Blonsky, I.; Beljonne, D.; Shuai, Z.; Bredas, J. L.; Arkhipov, V. I.; Heremans, P.; Emelianova, E. V.; Bässler, H. Singlet–Triplet Splitting of Geminate Electron–Hole Pairs in Conjugated Polymers. *Phys. Rev. Lett.* **2004**, *93*, 066803.
- (18) Uoyama, H.; Goushi, K.; Shizu, K.; Nomura, H.; Adachi, C. Highly Efficient Organic Light-Emitting Diodes from Delayed Fluorescence. *Nature* **2012**, *492*, 234–238.
- (19) Zhang, Q.; Li, J.; Shizu, K.; Huang, S.; Hirata, S.; Miyazaki, H.; Adachi, C. Design of Efficient Thermally Activated Delayed Fluorescence Materials for Pure Blue Organic Light Emitting Diodes. *J. Am. Chem. Soc.* **2012**, *134*, 14706–14709.
- (20) Nakanotani, H.; Masui, K.; Nishide, J.; Shibata, T.; Adachi, C. Promising Operational Stability of High-Efficiency Organic Light-Emitting Diodes Based on Thermally Activated Delayed Fluorescence. *Sci. Rep.* **2013**, *3*, 2127.
- (21) Zhang, Q.; Li, B.; Huang, S.; Nomura, H.; Tanaka, H.; Adachi, C. Efficient Blue Organic Light-Emitting Diodes Employing Thermally Activated Delayed Fluorescence. *Nat. Photonics* **2014**, *8*, 326–332.
- (22) Dias, F. B.; Bourdakos, K. N.; Jankus, V.; Moss, K. C.; Kamtekar, K. T.; Bhalla, V.; Santos, J.; Bryce, M. R.; Monkman, A. P. Triplet Harvesting with 100% Efficiency by Way of Thermally Activated Delayed Fluorescence in Charge Transfer OLED Emitters. *Adv. Mater.* **2013**, *25*, 3707–3714.
- (23) Miller, R. D.; Michl, J. Polysilane High Polymers. *Chem. Rev.* **1989**, *89*, 1359–1410.
- (24) Nespurek, S.; Eckhardt, A. Poly(silylene)s: Charge Carrier Photogeneration and Transport. *Polym. Adv. Technol.* **2001**, *12*, 427–440.
- (25) Harrah, L. A.; Zeigler, J. M. Electronic Spectra of Polysilanes. *Macromolecules* **1987**, *20*, 601–608.
- (26) Fujii, A.; Yoshimoto, K.; Yoshida, M.; Ohmori, Y.; Yoshino, K.; Ueno, H.; Kakimoto, M.; Kojima, H. Electroluminescent Diodes Utilizing Polysilanes. *Jpn. J. Appl. Phys.* **1996**, *35*, 3914–3917.
- (27) Ebihara, K.; Koshihara, S.; Miyazawa, T.; Kira, M. Polysilane-Based Polymer Diodes Emitting Ultraviolet Light. *Jpn. J. Appl. Phys.* **1996**, *35*, L1278–L1280.
- (28) Eckhardt, A. *Untersuchung der lichinduzierten elektrischen Leitfähigkeit von Polysilanen*; Fachbereich 5—Chemie, Technische Universität Berlin: Berlin, 1995.
- (29) Eckhardt, A.; Yars, N.; Wollny, T.; Schnabel, W.; Nespurek, S. Photoconductivity in Poly(biphenylmethylsilylene). *Ber. Bunsen-Ges. Phys. Chem.* **1994**, *98*, 853–857.
- (30) Frisch, M. J.; et al. *Gaussian09*, revision D.01; Gaussian Inc.: Wallingford, CT, 2013.
- (31) Parr, R. G.; Yang, W. *Density-Functional Theory of Atoms and Molecules*; Oxford University Press: Oxford, U.K., 1989.
- (32) Stephens, P. J.; Devlin, F. J.; Chabalowski, C. F.; Frisch, M. J. Ab Initio Calculation of Vibrational Absorption and Circular Dichroism Spectra Using Density Functional Force Fields. *J. Phys. Chem.* **1994**, *98*, 11623–11627.
- (33) Frisch, M. J.; Pople, J. A.; Binkley, J. S. Self-Consistent Molecular Orbital Methods 2S. Supplementary Functions for Gaussian Basis Sets. *J. Chem. Phys.* **1984**, *80*, 3265–3269.
- (34) Stratmann, R. E.; Scuseria, G. E.; Frisch, M. J. An Efficient Implementation of Time-Dependent Density-Functional Theory for the Calculation of Excitation Energies of Large Molecules. *J. Chem. Phys.* **1998**, *109*, 8218–8224.
- (35) Gordon, M. S.; Schmidt, M. W. Advances in Electronic Structure Theory: GAMESS a Decade Later. In *Theory and Applications of Computational Chemistry: The First Forty Years*; Dykstra, C. E., Frenking, G., Kim, K. S., Scuseria, G. E., Eds.; Elsevier: Amsterdam, 2005; pp 1167–1189.
- (36) Nakano, H.; Uchiyama, R.; Hirao, K. Quasi-Degenerate Perturbation Theory with General Multiconfiguration Self-Consistent Field Reference Functions. *J. Comput. Chem.* **2002**, *23*, 1166–1175.
- (37) Chiba, M.; Tsuneda, T.; Hirao, K. Excited State Geometry Optimizations by Analytical Energy Gradient of Long-Range Corrected Time-Dependent Density Functional Theory. *J. Chem. Phys.* **2006**, *124*, 144106.
- (38) Nespurek, S.; Kadashchuk, A.; Skryshevski, Yu. A.; Fujii, A.; Yoshino, K. Origin of Broad Visible Luminescence in Poly[methyl-(phenyl)silylene] Thin Films. *J. Luminesc.* **2002**, *99*, 131–140.
- (39) Nespurek, S.; Schauer, F.; Kadashchuk, A. Visible Photoluminescence in Polysilanes. *Monatsh. Chem.* **2001**, *132*, 159–168.
- (40) Burkhart, R. D.; Chakraborty, D. K. Binding Energies of Triplet Excimers in Poly(N-vinylcarbazole) Solid Films from Laser-Based Kinetic Spectroscopy between 15 and 55 K. *J. Phys. Chem.* **1990**, *94*, 4143–4147.
- (41) Belfield, K. D.; Bondar, M. V.; Morales, A. R.; Frazer, A.; Mikhailov, I. A.; Przhonska, O. V. Photophysical Properties and Ultrafast Excited-State Dynamics of a New Two-Photon Absorbing Thiopyranil Probe. *J. Phys. Chem. C* **2013**, *117*, 11941–11952.

- (42) Romanovskii, Yu. V.; Bässler, H. Phosphorescence from a Ladder-Type Conjugated Polymer in Solid Solutions at Low Temperature. *Chem. Phys. Lett.* **2000**, *326*, 51–57.
- (43) Patil, S. A.; Scherf, U.; Kadashchuk, A. New Conjugated Ladder Polymer Containing Carbazole Moieties. *Adv. Funct. Mater.* **2003**, *13*, 609–614.
- (44) Hertel, D.; Setayesh, S.; Nothofer, H.-G.; Scherf, U.; Müllen, K.; Bässler, H. Phosphorescence in Conjugated Poly(*para*-phenylene)-Derivatives. *Adv. Mater.* **2001**, *13*, 65–70.
- (45) Hertel, D.; Bässler, H.; Guentner, R.; Scherf, U. Triplet-Triplet Annihilation in a Poly(fluorene)-Derivative. *J. Chem. Phys.* **2001**, *115*, 10007–10013.
- (46) Wayne, R. P. *Principles and Applications of Photochemistry*; Oxford University Press: Oxford, U.K., 1988.
- (47) Turro, N. J. *Modern Molecular Photochemistry*; University Science Books: Sausalito, CA, 1991.
- (48) Schueppel, R.; Ullrich, C.; Pfeiffer, M.; Leo, K.; Brier, E.; Reinold, E.; Baeuerle, P. Enhanced Photogeneration of Triplet Excitons in an Oligothiophene-Fullerene Blend. *ChemPhysChem* **2007**, *8*, 1497–1503.
- (49) McGlynn, S. P.; Azumi, T.; Kinoshita, M. *Molecular Spectroscopy of the Triplet State*; Prentice-Hall: Englewood Cliffs, NJ, 1969.
- (50) Difley, S.; Beljonne, D.; van Voorhis, T. On the Singlet–Triplet Splitting of Geminate Electron–Hole Pairs in Organic Semiconductors. *J. Am. Chem. Soc.* **2008**, *130*, 3420–3427.
- (51) Clarke, T. M.; Durrant, J. R. Charge Photogeneration in Organic Solar Cells. *Chem. Rev.* **2010**, *110*, 6736–6737.
- (52) Kanemitsu, Y.; Suzuki, K. Visible Photoluminescence from Silicon-Backbone Polymers. *Phys. Rev. B* **1995**, *51*, 13103–13110.
- (53) Islangulov, R. R.; Lott, J.; Weder, C.; Castellano, F. N. Noncoherent Low-Power Upconversion in Solid Polymer Films. *J. Am. Chem. Soc.* **2007**, *129*, 12652–12653.
- (54) Endo, A.; Ogasawara, M.; Takahashi, A.; Yokoyama, D.; Kato, Y.; Adachi, C. Thermally Activated Delayed Fluorescence from Sn<sup>4+</sup>-Porphyrin Complexes and Their Application to Organic Light Emitting Diodes—A Novel Mechanism for Electroluminescence. *Adv. Mater.* **2009**, *21*, 4802–4806.
- (55) Forget, S.; Chenais, S. *Organic Solid-State Lasers*; Springer Series in Optical Sciences 175; Springer-Verlag: Berlin, Heidelberg, 2013.
- (56) Fishchuk, I. I.; Kadashchuk, A.; Bässler, H.; Nespurek, S. Nondispersive Polaron Transport in Disordered Organic Solids. *Phys. Rev. B* **2003**, *67*, 224303.